

# Single-crystal piezoceramic actuation for dynamic stall suppression

D. Thakkar\*, R. Ganguli

Indian Institute of Science, Department of Aerospace Engineering, Bangalore 560 012, India

Received 29 May 2005; received in revised form 4 January 2006; accepted 16 January 2006

Available online 9 March 2006

## Abstract

PZN-8%PT(111)—a new single-crystal piezoceramic is explored for its potential to torsionally actuate the existing structure utilizing the induced shear mechanism of piezoceramics. A model of the elastic rotor blade and piezoceramic actuator is developed using the Hamilton's principle and the resulting equations are solved using the finite element method. Numerical results show that the single crystal material is able to generate sufficient amount of torsion to enable suppression of high blade section angle of attack existing in stalled regions of a helicopter rotor at high speed forward flight. The suppression of dynamic stall leads to considerable improvement in helicopter performance. Thus, PZN-8%PT(111) could be proposed for investigation in applications demanding high actuation authority and for alleviating the dynamic stall related problems which limit helicopter performance in high speed flight.

© 2006 Elsevier B.V. All rights reserved.

**Keywords:** Single crystal; Piezoceramics; Dynamic stall; Actuation

## 1. Introduction

Typical piezoelectric materials (PZTs) may have stroke limitations in the applications that demand higher stroke/actuation authority. Also, there are limits to the use of high electric fields to increase actuator authority due to increasing complexity and bulky nature of the required electronic equipment and the risk of depoling. Addressing this issue, in the 1990s attention was directed towards relaxor-PT systems which were found to have many advantages over the conventional piezoceramic materials. The principal advantage was the ease with which these piezoelectric single crystals could be grown. Generally, if the appropriate axis orientation is utilized, single crystals are found to have superior properties than ceramics [1]. Orientations can be tailored to optimize response to longitudinal, transverse and shear excitations commonly used in transducer designs. A significant reorientation of domains is achieved during polarization of single crystal materials, resulting in higher electromechanical coupling factors (applied electrical energy is converted into mechanical or acoustic energy) of 90% or more, as compared to 70% for polarized conventional piezoceramics. Single crystal piezoelectric materials also offer higher bandwidths, up to

135%, as compared to 40–45% for PZT. In actuator applications, single crystal materials can achieve field-induced strains three times greater than those obtained in PZT. The dielectric losses in single crystals are much less than 1%, as compared to 2% for PZT.

The maximum strain energy density of an actuator should be as high as possible for aiming at an optimum performance of the actuator [2]. Generally, for an actuator's performance the induced strain due to the applied field is the most important parameter and this is also reflected in the strain energy density function which can be defined as below:

$$e_{\max} = \frac{1}{\rho} \left( \frac{1}{4} \right) \left( \frac{1}{2} \right) E (s_{\max}^2) \quad (1)$$

where  $e_{\max}$  is the strain energy density,  $E$  the elastic modulus of the actuator,  $s_{\max}$  the maximum field induced strain and  $\rho$  is the actuator's density. The factor 1/4 in Eq. (1) is appropriate for an actuator impedance related to its surroundings. In general, PZN-PT ceramics are found to have a very high strain energy density (approximately 10 times of PZT ceramics).

Piezoelectric properties of PZN-PT type single crystals with (0 0 1)-orientation have been found to possess large direct piezoelectric coefficients ( $d_{33}$ ,  $d_{31}$ ) which are almost of the order of 10 times that of a soft piezoceramic like PZT-5H. However, the shear coefficient,  $d_{15}$  of these materials is relatively poor as compared to soft piezoceramics like PZT-5H and their applications

\* Corresponding author.

E-mail addresses: [dipali@aero.iisc.ernet.in](mailto:dipali@aero.iisc.ernet.in) (D. Thakkar), [ganguli@aero.iisc.ernet.in](mailto:ganguli@aero.iisc.ernet.in) (R. Ganguli).

have been limited to those requiring direct strain. Recently, Liu et al. [3] reported that the piezoelectric shear coefficient  $d_{15}$  of PZN-4.5%PT and PZN-8%PT crystals oriented in  $\langle 111 \rangle$  is very high as compared to the conventional soft piezoceramic materials. At the same applied electric field, PZN-8%PT was found to have a much higher  $d_{15}$  than PZT-5H. Thus, PZN-8%PT was proposed to be a promising material for applications involving shear transducers [3]. The shear mode properties of these lead based single crystals have also been investigated by [4]. PZN-8%PT is linear within the range of 210 V/mm. For this material,  $d_{15}$  is calculated to be  $18,750\text{e-}9\text{ mm/V}$  (at 200 V). This value is almost 10 times the value of  $d_{15}$  for PZT-5H at 400 V and 13 times the value at 200 V. The Young's modulus of PZN-8%PT is almost double as that of aluminum and PZT-5H. Density is marginally higher as compared to that of PZT-5H. A detailed characterization of the electromechanical properties of relaxor-PT single crystal ceramics is given in [5]. Large size single crystals are now commercially available at reduced costs [6].

In this paper, piezoelectric single crystal-PZN-8%PT oriented in  $\langle 111 \rangle$  direction is used to generate induced shear actuation for suppressing dynamic stall in helicopter rotors. Dynamic stall is characterized by flow separation over the airfoil leading to a sudden loss in lift and increase in drag and pitching moment which results in severe deterioration in helicopter performance. Stall occurs in the retreating blade when the rotor is moving with a forward speed. In forward flight the velocity distribution over the blades is not uniform and the blade moving into the wind experiences greater velocities than the blade retreating away from the wind. This results into non-uniform blade section angle of attack distributions over the blade. This asymmetry of the aerodynamic environment in forward flight is due to the combination of the forward velocity and rotor rotation. It is also important to mention that in general, for a four-bladed rotor 2/rev control is found to be beneficial for reducing stall area and 3, 4 and 5/rev control for reducing vibration [7]. Here  $N/\text{rev}$  control implies actuating the blade at harmonics of  $N\Omega$  where  $\Omega$  is the rotation speed. For a typical rotor with  $\Omega = 5\text{ Hz}$ , 2/rev (2P) implies actuating the blade at a frequency of 10 Hz. Such control can be provided using piezoelectric actuators which have high bandwidth.

To the best of authors knowledge, the only study using piezoceramic actuation for dynamic stall suppression was done by Wilkie et al. [8]. They used the active fiber composite (AFC) approach to suppress dynamic stall. AFC laminae were embedded in the blade structure at alternating  $\pm 45^\circ$  orientation angles. Classical laminated plate theory was used for deriving structural and piezoelectric actuation properties. In this study, 2/rev control was used to suppress the stall area on the rotor disk. However, it should be noted that even AFC's being built using early piezoceramic materials were very limited in terms of actuation capability. The full potential of smart actuation was therefore not exploited. The current study addresses this problem by using the recently explored single crystal piezoceramic; PZN-8%PT  $\langle 111 \rangle$ -induced shear actuation for reducing the stall area and blade section angle of attack in the stalled regions.

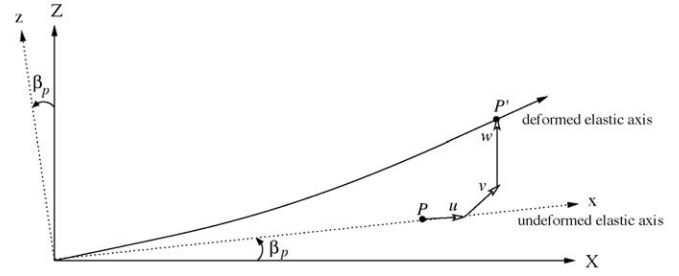


Fig. 1. Deformation of rotor blade.

## 2. Formulation and modeling

The generic governing differential equations are derived for a smart beam/rotor blade undergoing axial, chord-wise bending, span-wise bending and elastic twist and supporting axial, bending and torsion actuation, using Hamilton's principle. A point P on the undeformed elastic axis undergoes deflection  $u$ ,  $v$ ,  $w$  in the  $x$ ,  $y$ ,  $z$  and moves to a point P' as shown in Fig. 1.  $X$  and  $Y$  are the hub coordinate axes and blade is at a precone angle  $\beta_p$  from the hub axes. The cross section undergoes a rotation  $\theta_1 = \theta_0 + \hat{\phi}$ . Here  $\hat{\phi}$  is the elastic twist and  $\theta_0$  is given as  $\theta_0 = \theta_{75} + \theta_{tw}(\frac{x}{R} - 0.75) + \theta_{1c} \cos \psi + \theta_{1s} \sin \psi$ . Here,  $\theta_{75}$  is the blade pitch at 75% span of blade,  $\theta_{tw}$  is the blade linear pretwist and  $\theta_{1s}$  and  $\theta_{1c}$  are cyclic pitch controls.

The constitutive equations of an isotropic beam plate [9] can be written as follows:

$$\begin{Bmatrix} \epsilon_{xx} \\ \epsilon_{\eta\eta} \\ \epsilon_{\zeta\zeta} \\ \epsilon_{x\eta} \\ \epsilon_{\eta\zeta} \\ \epsilon_{x\zeta} \end{Bmatrix} = \begin{bmatrix} 1/E & -\nu/E & -\nu/E & 0 & 0 & 0 \\ -\nu/E & 1/E & -\nu/E & 0 & 0 & 0 \\ -\nu/E & -\nu/E & 1/E & 0 & 0 & 0 \\ 0 & 0 & 0 & 1/G & 0 & 0 \\ 0 & 0 & 0 & 0 & 1/G & 0 \\ 0 & 0 & 0 & 0 & 0 & 1/G \end{bmatrix} \begin{Bmatrix} \sigma_{xx} \\ \sigma_{\eta\eta} \\ \sigma_{\zeta\zeta} \\ \tau_{x\eta} \\ \tau_{\eta\zeta} \\ \tau_{x\zeta} \end{Bmatrix} \quad (2)$$

The following fundamental assumptions are made for the analysis [10]:

- (1) mid-line of a plate segment does not deform in its own plane;
- (2) the normal stress in the contour direction,  $\sigma_{\eta\eta}$  is neglected relative to the normal axial stress  $\sigma_{xx}$ ;
- (3) rotor blade is a long slender beam and hence the uniaxial stress assumptions can be made;  $\sigma_{\eta\eta} = 0$ ,  $\sigma_{\zeta\zeta} = 0$  and  $\tau_{\eta\zeta} = 0$ .

The strain displacement field (accurate up to second order and accounting for moderate deflections) is defined as [10];

$$\begin{aligned} \epsilon_{xx} = & u' + \frac{v'}{2} + \frac{w'^2}{2} - \lambda_T \phi'' + (\eta^2 + \zeta^2)(\theta'_0 \phi' + \phi^2/2) \\ & - v''[\eta \cos(\theta_0 + \hat{\phi}) - \zeta \sin(\theta_0 + \hat{\phi})] \\ & - w''[\eta \sin(\theta_0 + \hat{\phi}) + \zeta \cos(\theta_0 + \hat{\phi})] \end{aligned} \quad (3)$$

$$\epsilon_{x\eta} = -(\zeta + \lambda_{T,\eta})\phi' = -\hat{\zeta}\phi' \quad (4)$$

$$\epsilon_{x\zeta} = (\eta - \lambda_{T,\zeta})\phi' = \hat{\eta}\phi' \quad (5)$$

Download English Version:

<https://daneshyari.com/en/article/737566>

Download Persian Version:

<https://daneshyari.com/article/737566>

[Daneshyari.com](https://daneshyari.com)